

Extraction of glucomannan from porang (*Amorphophallus muelleri* Blume) with freeze-thaw cycles pre-treatment

Enny SHOLICHAH^{1,2} , Bambang PURWONO^{1*} , Agnes MURDIATI³ ,
Akhmad SYOUFIAN¹ , Achmat SARIFUDIN² 

Abstract

Amorphophallus muelleri Blume tuber, which is called porang in Indonesia, is one of the biggest glucomannan sources next to the konjac tuber. Glucomannan is commonly produced by ethanol extraction technique. This study aimed to propose the freeze-thaw cycles (FTC) pre-treatments with two factors including freezing time and the number of cycles before the glucomannan extraction step and investigated the impact on the physicochemical and morphological properties of the extracted glucomannan. The obtained data were statistically tested by means of multivariate analysis of variance (MANOVA) and post-hoc Duncan tests at a significance level (*P*) of 0.05. The treated samples were statistically compared with the control sample (without FTC) by means of the Dunnett's test. The result showed that FTC pre-treatments changed the morphology of glucomannan from smooth to become porous globes showing more fissures on its surface. Generally, the freezing time treatments affected the physicochemical properties of glucomannan except for its protein and calcium oxalate contents. The number of cycles did not significantly affect the protein, starch, and calcium oxalate contents. The Dunnett's test results indicated that the ash, carbohydrate (glucomannan), and color of the glucomannan obtained by the FTC pre-treatments were significantly different from those of the control sample.

Keywords: glucomannan; extraction; freeze-thaw cycles pre-treatments; porang; physicochemical-morphological properties.

Practical Application: the freeze-thaw pre-treatment method is potential to be implemented in glucomannan extraction industry.

1. Introduction

Glucomannan is a polysaccharide substance widely used in the food and pharmaceutical industries due to its health benefits and its capability to improve the texture of a product (Yao-ling et al., 2013). *Amorphophallus muelleri* Blume tuber, which is named porang in Indonesia, contains about 6–20% of glucomannan; therefore, it can be a potential source of glucomannan (Dwiyono & Djauhari, 2019).

Glucomannan can be extracted from fresh tubers or porang flour by using wet and dry extraction methods. The dry extraction method uses simple mechanical treatments such as a stamp mill or ball mill, followed by a cyclone separation technique. However, the dry extraction methods produce quite low glucomannan content (56–67%), high starch content (3.09%), and high calcium oxalate content (3.23%) (Faridah et al., 2012; Widjanarko et al., 2015). Meanwhile, the wet extraction method produces a high yield of glucomannan (79.19%), a high starch content (2.69%), and relatively low calcium oxalate content (0.8%) (Faridah & Widjanarko, 2013; Wardhani et al., 2015).

However, the wet extraction method uses high-cost organic solvents, especially alcohol substances such as ethanol and isopropyl alcohol. Moreover, the quality of glucomannan flour produced by the wet extraction method is influenced by extraction parameters such as the extraction temperature, solvent concentration, and volume of solvent (Chua et al., 2012; Nurlela et al., 2020; Wardhani et al., 2015). Therefore, since both methods have their own limitations, research is still needed to obtain the optimum glucomannan extraction method to produce high glucomannan content and, at the same time, low impurities.

Other goals in developing the glucomannan extraction method of *Amorphophallus* flour are to reduce starch, protein, ash, and oxalate contents in order to fulfill the standard requirement of pure glucomannan flour. The common steps in glucomannan extraction include preparation of porang chips and flour, solvent extraction, and glucomannan purification (Shi et al., 2020b). Chua et al. (2013) reported that glucomannan globes are deposited in idioblast cells of parenchyma tissue. The glucomannan cells are usually 15 times bigger than starch

Received: 9 Jan., 2023

Accepted: 12 Apr., 2023

¹Universitas Gadjah Mada, Faculty of Mathematics and Natural Science, Department of Chemistry, Sekip Utara, Jl. Bulaksumur, Yogyakarta, Indonesia.

²Republic of Indonesia, National Research and Innovation Agency, Research Center for Appropriate Technology, Jl. KS, Tubun No. 5 Subang, West Java, Indonesia.

³Universitas Gadjah Mada, Faculty of Agriculture Technology, Department of Food and Agriculture Product Technology, Jl. Flora No.1, Bulaksumur, Yogyakarta, Indonesia.

*Corresponding author: purwono.bambang@ugm.ac.id

granules; therefore, they can be separated from starch granules and oxalate compounds by means of the weight or size differentiation methods (Chua et al., 2013; Peiying et al., 2003).

Generally, starch granules in plant tissues can be destroyed by freezing during the ice crystal forming and growing cycles (Yang et al., 2021). Furthermore, ice crystallization causes destruction of the texture of plant tissues (van der Sman, 2020). A slow freezing rate (-20°C) produces bigger ice crystals than a medium freezing rate (-40°C) or fast freezing rate (-80°C). Moreover, freezing-thawing cycles (FTC) have the ability to break hydrogen bonds in the inter- and intra-hydroxyl groups of polysaccharide and protein compounds (Feng et al., 2022; Xu et al., 2022). For instance, the FTC reduces the molecular weight of gluten (Zhao et al., 2013), implying a depolymerization process of a high-molecular-weight protein into peptides. Based on these results, FTC treatment shows a promising method to be explored in the glucomannan extraction process from porang tuber.

Freezing-thawing pre-treatments have also been reported as a physical method to assist wet extraction methods. FTC increases the tissue's damage, which can facilitate the release of extracellular components during the thawing process. FTC pre-treatments have been applied in pectin extraction from mango (Charoenrein & Owcharoen, 2016), gelatin extraction from skin fish (Feng et al., 2021), and polysaccharide extraction from taro (Anwar et al., 2021). FTC has also been reported to affect the microstructural and physicochemical properties of the extracted components (Abedi et al., 2022). Since the FTC pre-treatments have not been utilized to assist the glucomannan extraction process from porang tuber, this study aims to investigate the impact of the FTC pre-treatments on the physicochemical (color, viscosity, swelling properties, proximate, starch, Ca-oxalate, glucomannan, Fourier transform infrared spectrophotometry, and X-ray diffraction pattern) and morphological properties of the glucomannan flour prepared by the wet extraction process.

2. Materials and methods

2.1. Materials

The *Amorphophallus* tubers were obtained from a local porang farmer in Subang, West Java, which were harvested in 2 years. The chemicals were ethanol (95%), enzymes of amylase and amyloglucosidase, HCl (37%), KMnO_4 , H_2SO_4 (98%), and phenolphthalein.

2.2. Freezing-thawing cycles pre-treatment

The *Amorphophallus* tubers were washed, peeled, and sliced to a size of ± 3 mm, and then the chips were packed in a plastic bag (800 g/pack). The samples were frozen at -20°C for 2, 4, and 6 days and then thawed at 4°C. The freezing-thawing treatment was repeated for 1, 2, 3, and 4 cycles. The chips were dried by using a cabinet dryer at a temperature of 50°C, and then they were milled and sieved to 40 mesh. The porang flour was subjected to ethanol extraction steps (ethanol of 40% (v/v), flour to ethanol ratio of 1:5, and two extraction times) to produce the glucomannan flour. The wet glucomannan flour was then dried

in a cabinet dryer at a temperature of 50°C. The dried flour was milled and sieved to 40 mesh. Prior to analysis, samples were stored in a leak-proof box containing silica gel and kept at room temperature. The sample that did not undergo freezing-thawing pre-treatment was prepared as the control sample.

2.3. Proximate and starch determination

The proximate and starch content of the sample were determined according to the method of National Food and Beverage Analysis (National Standardization Agency, 1992). The moisture and ash contents were measured using the gravimetric method. Protein content was assayed by a nitrogen combustion method using a Buchi-Dumaster D480-Germany. The protein content was calculated by using a nitrogen conversion factor of 5,7 according to the standards of the U.S. Food Chemical Codex (FCC) and the European Commission (Chua et al., 2012). The percentage of carbohydrate (glucomannan) was calculated using a different method (FAO, 1996). The starch content was determined based on the enzymatic method of Chua et al. (2012) with modifications.

2.4. Oxalate content

The total oxalate in the samples was measured by the volumetric permanganometry method by Sulaiman et al. (2020). A sample (1 g) was dispersed with distilled water (95 mL) in a 250-mL Erlenmeyer. Then, 5 mL of HCl (6 M) was added and heated for 1 h at 100°C. After cooling to room temperature, distilled water was added to the suspension up to a volume of 125 mL. The sample was then filtered with Whatman filter paper of size 42. The filtrate (50 ml) was diluted with distilled water until it reached a volume of 150 mL. H_2SO_4 (20%) with a volume of 10 mL was added to the sample, then heated until boiled. The sample was titrated with KMnO_4 at 0.05 M until the color of the solution became pink, which lasted for 30 s. The total oxalate content of the sample was calculated by the Equation 1:

$$\text{Calcium oxalate} \left(\frac{\text{mg}}{100 \text{ g}} \right) = \frac{V_{\text{KMnO}_4} \times 0.00225 \times df \times 10^5}{W \text{ sample} (g) \times 5} \quad (1)$$

Where:

W sample: the weight of the sample;

Df: the dilution factor (2.5 is obtained from the volume of the filtrate of 125 mL divided by the volume of filtrate used of 50 mL);

0.00225: the mass volume equivalent constant (1 mL KMnO_4 0.05 M is equivalent to 0.00225 g of anhydrous oxalic acid);

5: the molar equivalent of KMnO_4 .

2.5. Color

The color of the samples was measured using a colorimeter (3NH-Taiwan). The sample was placed in a standard cuvette, and then the color reading was carried out. Three color parameters, namely, L^* (lightness index), a^* (red to green index), and b^* (yellow to blue index), were reported.

2.6. Viscosity

The viscosity of the glucomannan sample was determined according to the method of Yanuriati et al. (2017). Glucomannan suspension of 1% (w/w) was stirred for 60 min at 350 rpm until evenly mixed. The viscosity of the sample was measured using a viscometer (Brookfield Viscometer Model LVTDV-II, USA) at room temperature using an appropriate spindle and speed.

2.7. Swelling power

The swelling power of the glucomannan sample was measured according to the method of Tao et al. (2018) with some modifications. The glucomannan suspension (1% w/v) was prepared in a centrifuge tube, then heated in a shaking water bath at 80°C for 30 min, cooled for 5 min, and centrifuged at 3,000×g for 15 min. The supernatant was discharged, and the sediment was weighted. The swelling power (SP, g/g) was calculated based on the Equation 2:

$$\text{Swelling power (\%)} = \frac{\text{The weight of sediment (g)}}{\text{The dry weight of sampel (g)}} \times 100\% \quad (2)$$

2.8. Swelling capacity

The swelling capacity of the sample was determined according to the method of Felix da Silva et al. (2020) with some modifications. The sample (0.2 g) was placed in a scaled test tube, and then 10 mL of distilled water was added. The mixture was stored at room temperature for 18 h, and the final volume after soaking was recorded. The swelling capacity value was calculated based on the Equation 3:

$$\text{Swelling capacity (ml/g)} = \frac{\text{Volume after soaking (ml)}}{\text{Weight of sampel (g)}} \quad (3)$$

2.9. Morphological analysis

The morphological properties of samples were observed by a JEOL JSM-IT200 Scanning Electron Microscope (Japan). Before the analysis, the sample was sieved through an 80-mesh opening. The sample was mounted on a metal stub that had previously been covered with double-sided adhesive tape. The excess sample was removed by spraying it with nitrogen. Then, it was coated with gold and examined with an accelerating voltage of 2 kV. The samples were observed with 100-, 500-, and 1,000-times magnifications.

2.10. Molecular weight

The molecular weight distribution of glucomannan was measured based on the method of Kurt and Kahyaoglu (2017) using the Gel Permeation Chromatography/Size Exclusion Chromatography (GPC/SEC) system (Agilent Technologies, 1260 Infinity II, UK) with multiple detectors: a UV detector (Agilent 1260 Infinity II) and a refractive index (RI) detector (Agilent 1,260 Infinity II). Water with the addition of 0.02% NaN₃ was used as the mobile phase. The sample was dissolved in water (1 mg/mL), stirred and filtrated using Millipore 0.45 µL. The flow rate was 0.5 mL/min, and the columns and detectors were maintained at 35°C.

2.11. FTIR

FTIR-BRUKER ALPHA II was employed to observe the functional groups of glucomannan. The analysis was carried out within the infrared region of wave number 400–4,000 cm⁻¹ with a resolution of 4 cm⁻¹.

2.12. X-Ray Diffraction

The X-ray diffraction patterns of the glucomannan samples were obtained by using an XRD instrument (Panalytical X'pert 3 Powder, UK). The samples were scanned at a diffraction angle (2θ) of 5°–70°. The method of Kurt and Kahyaoglu (2017) was followed to analyze the XRD data.

2.13. Statistical analysis

A completely randomized design (CRD) with two factors including the freezing time (2 days (F2), 4 days (F4), and 6 days (F6)) and freezing cycles (1 cycle (S1), 2 cycles (S2), 3 cycles (S3), and 4 cycles (S4)) (Table 1) was used to study the effect of freezing-thawing pre-treatments on the observed parameters including the proximate, starch, calcium oxalate, color, viscosity, swelling properties, FTIR, and XRD. Multivariate variance analysis (MANOVA) and the post-hoc Duncan test were performed to test the significant differences between the mean values of each treatment. The statistical significance level (*P*) was set at 0.05. The data of the treated samples were statistically compared with those of the control sample (without FTC) by means of the Dunnett's test.

3. Results and discussion

3.1. Proximate, starch, and oxalate contents

The effects of FTC pre-treatments on the removal of impurities (ash, protein, glucomannan, calcium oxalate, and starch) during the glucomannan extraction process are summarized in Figure 1. The FTC pre-treatments affected the moisture, ash, glucomannan, and starch contents of the glucomannan flour, but not its protein and oxalate contents. The moisture content of glucomannan samples ranged from 6.13 to 12.07%. Figure 1A indicates that the moisture content of glucomannan flour was influenced by the freezing time but not by the freezing-thawing cycle. The moisture content of samples frozen for 4 and 6 days was less than 10%, which satisfies the standard for purified glucomannan (Peiying et al., 2002). The longer freezing time resulted in a lower moisture content. During freezing, ice crystals grow within the intracellular and extracellular structures of wet porang chips. The growth of ice crystals may destroy the tissues

Table 1. The research design of FTC pre-treatment for glucomannan extraction.

Freezing Time	Cycle of Freezing-Thawing			
	S1	S2	S3	S4
F2 (2 days)	1 cycle	2 cycles	3 cycles	4 cycles
F4 (4 days)	1 cycle	2 cycles	3 cycles	4 cycles
F6 (6 days)	1 cycle	2 cycles	3 cycles	4 cycles

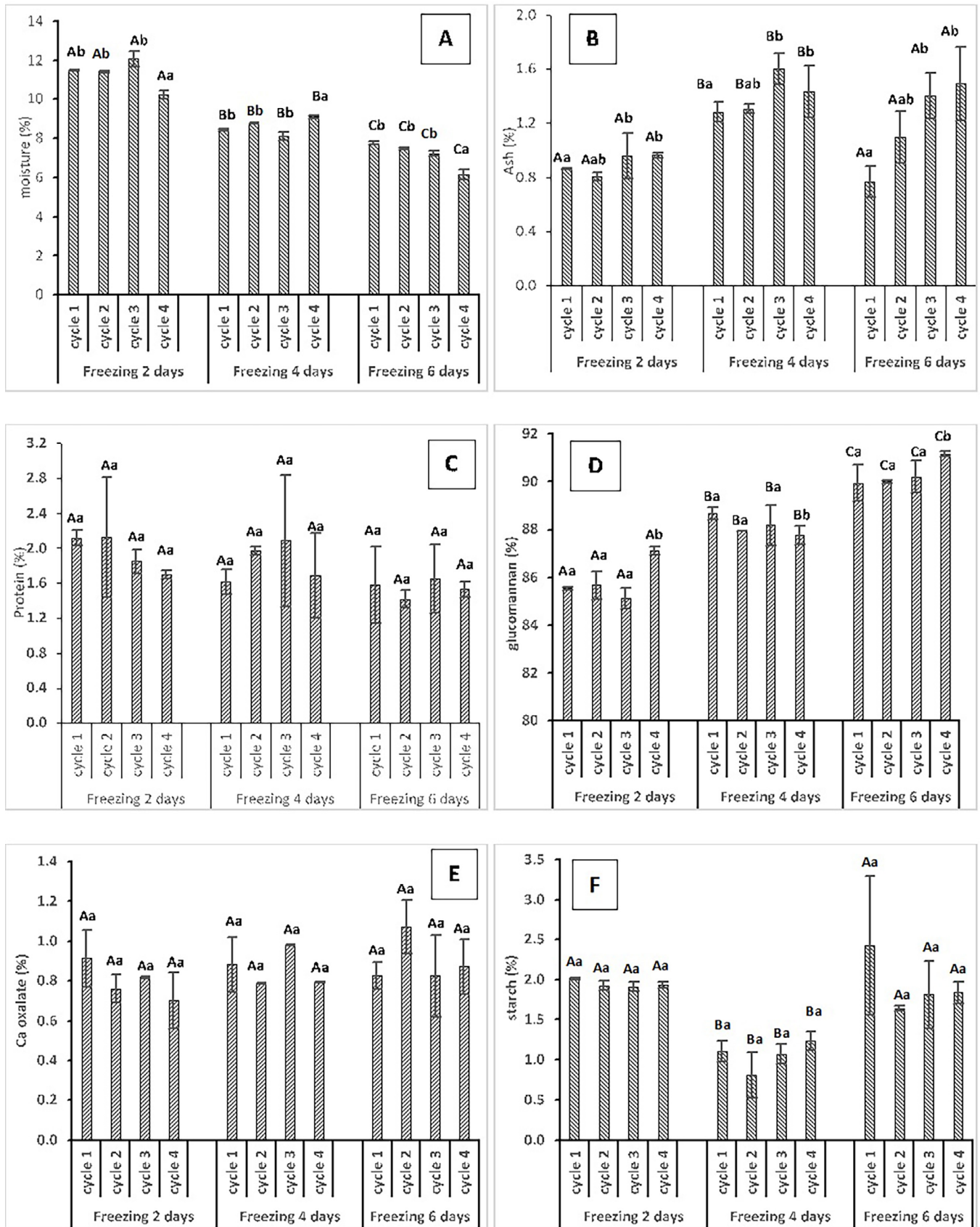


Figure 1. Chemical composition of samples: (A) moisture content; (B) ash; (C) protein; (D) carbohydrate/glucomannan; (E) calcium oxalate; and (F) starch. Description: The average value marked by different letter notations showed a noticeable difference according to further tests of Duncan at a real level of 5%. Capital letter notation is read for freezing time, and lowercase notation is read for cycle.

of the sliced porang, forming porous structures. Finally, during the drying process, the water is easily evaporated and escapes from the inside structures, passing through the porous structures toward the surrounding environment. This mechanism was also reported to occur during the drying of the sliced potato pre-treated with freezing-thawing cycles (Shen et al., 2020). Moreover, the severity of tissue damage may increase with a longer freezing time. Freezing at -20°C with a slow freezing time causes greater tissue damage than freezing at -40 and -80°C . The effect of freezing temperature on the characteristics of the material has been reported by previous researchers (Charoenrein & Owcharoen, 2016; Phothiset & Charoenrein, 2014). Results of the Dunnett's test indicate the moisture content of FTC-treated samples (Supplementary Tables 1 and 2).

Results showed that the ash content of glucomannan flour was influenced by the freezing time and cycle. The ash content of glucomannan flour ranged from 0.77 to 1.49% (Figure 1B). The ash content of glucomannan flour obtained in this study was lower than that of non-FTC treatments, which were previously reported by Nurlela et al. (2020). The growth of ice crystals during FTC has the ability to destroy the tissue of porang chips, resulting in changes in its texture (Tu et al., 2015). This might assist in releasing some components, including minerals, during the glucomannan extraction process. The release of minerals during the glucomannan extraction process might result in a lower ash content in the remaining glucomannan flour. However, the result of the Dunnett's test showed that the ash content of the treated sample did not show a significant difference from that of the control sample (Supplementary Table 1).

Results indicated that the FTC pre-treatments did not significantly alter the protein content of glucomannan flour (Figure 1C). Moreover, the protein content of glucomannan flour obtained in this study was slightly lower than that of glucomannan flour obtained by the common extraction method (Nurlela et al., 2019, 2020). The protein content of glucomannan flour after 2- and 4-day freezing was slightly higher than that of the control flour. However, the protein content of glucomannan flour from different freezing cycles was not significantly different from that of the control sample ($P>0.05$). These results might indicate that cross-linking and oxidation reactions occur between proteins and other substances in the porang matrix during FTC pre-treatments (Zhang et al., 2017). These reactions cause the protein to bind to those components. Hence, it is difficult to be released from the porang matrix during the glucomannan extraction process.

Figure 1D shows that the glucomannan content was affected by the freezing time and the number of freezing-thawing cycles.

The highest glucomannan content was obtained from the FTC pre-treatments with the longest freezing time and the highest freezing-thawing cycles (6 days of freezing time and 4 cycles of freezing-thawing). The growth of ice crystals may reach its maximum size at the longest freezing time and the highest freezing-thawing cycles (Tao et al., 2015). The maximum growth of ice crystals may cause the maximum destruction of porang matrix, therefore assisting the release of glucomannan during the extraction process. FTC treatments may cause disruptions of the hydrogen bonds of a matrix, which lead to component dissolution and degradation (Feng et al., 2022).

Calcium oxalate is a natural substance that exists in porang tuber and causes irritation when it is in contact with the skin or tongue (Chairiyah et al., 2016; Noonan, 1999). Therefore, it is necessary to remove this substance during the glucomannan extraction process. The result shows that the FTC pre-treatments did not significantly affect the oxalate content of glucomannan flour (Figure 1D). The oxalate content of glucomannan flour from FTC pre-treatments ranged from 0.6 to 1.20%, which was lower than the previous study (1.35%) (Nurlela et al., 2019). Moreover, the result of the Dunnett's test (Supplementary Table 1) indicated that the oxalate content in glucomannan flour from the treated samples was not significantly different from that of the control sample. This might indicate the calcium oxalate is located in the intercellular matrix of porang tissue (Chua et al., 2013); therefore, the leaching of calcium oxalate during the glucomannan extraction process is not affected by the disrupted tissues caused by FTC pre-treatments.

Results showed that a freezing time of 4 days tended to produce glucomannan with the lowest starch content (Figure 1F). This indicates that 4 days of freezing time is the optimum time for ice to grow and disrupt the inter- and intracellular matrix of porang (Yu et al., 2022); therefore, the starch easily escapes from the broken tissues during the glucomannan extraction process.

Based on the result of this study, it can be summarized that the glucomannan flour produced by FTC pre-treatments satisfies the standard of glucomannan flour issued by FAO, the Professional Standard of the People's Republic of China and the European Food Safety Authority (Table 2). FAO and the Professional Standard of the People's Republic of China classified glucomannan as a food ingredient, but the European Food Safety Authority defined glucomannan as a food additive (FAO, 1996; Mortensen et al., 2017; Peiying et al., 2002). They specified different components and values for glucomannan, especially for the impurity's contents such as protein, ash, and starch (Table 2). The impurity content obtained in this study was lower than that observed in the previous study (Nurlela et al., 2019,

Table 2. The components of konjac glucomannan.

Component	FAO*	Professional Standard of the People's Republic**	European Food Safety Authority***	Our Results
Moisture	$\leq 15\%$	$\leq 11\%$	–	6.13%–12.07%
Ash	$\leq 5\%$	$\leq 4.5\%$	$\leq 2\%$	0.77%–1.60%
Protein	$\leq 8\%$	–	$\leq 1.5\%$	1.42%–2.12%
Starch	–	–	$\leq 1.5\%$	0.81%–2.43%
Glucomannan	$\geq 75\%$	$\leq 70\%$	$\geq 75\%$	85.13%–91.16%

*FAO (1996); **Peiying et al. (2002); ***Mortensen et al. (2017).

2020). Therefore, glucomannan obtained from FTC pre-treatments can be recommended as a food ingredient and additive in the food industries.

3.2. Color

The color of glucomannan flour was significantly influenced by the FTC pre-treatments ($P < 0.05$) (Table 3). Increasing the freezing time and the number of freezing-thawing cycles tended to change the color of glucomannan flour to a light brown. Furthermore, the Dunnett's test indicated that the treated samples tended to have a lighter color than the control sample. In the general glucomannan extraction process, the color of glucomannan flour becomes darker during drying (Shenglin et al., 2020). This is due to the browning reaction between browning enzymes, i.e., polyphenol oxidase, which exists in the porang tuber (Zhao et al., 2010), and its substrates, which occur in the presence of oxygen and at an elevated temperature. During FTC pre-treatments, the browning enzymes might be partially destroyed. Thus, the FTC pre-treatment prevents browning reactions from occurring during the glucomannan extraction process. Finally, the color of glucomannan flour produced from FTF pre-treatments can be maintained at a light brown.

3.3. Viscosity and swelling properties

The viscosity of the treated samples is summarized in Table 4. The viscosity of the control sample was 21,830 cP (Supplementary Table 2), whereas those of the treated samples ranged from 1,150 to 9,245 cP. These results indicated that the FTC pre-treatments indeed changed the viscosity of the treated samples. Generally, as the freezing time and cycle increased, the viscosity of the treated samples decreased. The decrease in viscosity can be associated with the decrease in molecular weight of glucomannan and the alteration of the polydispersity index (Ma et al., 2019; Shi et al., 2020a). Moreover, Jiang et al. (2018) also emphasize that depolymerization causes a decrease

in the viscosity of konjac glucomannan. FTC pre-treatments may destroy the hydrogen bonds among the glucomannan chains, resulting in the degradation of long chains of glucomannan. Finally, the degraded glucomannan chains exhibit lower viscosity than the normal glucomannan chains (Feng et al., 2022).

The data on swelling properties, including swelling power and swelling capacity, are presented in Table 4. The swelling power and swelling capacity of the treated samples ranged from 2,690 to 4,000% and 48.8 to 53.6 g/mL, respectively. Results indicated that the swelling properties of the treated samples were not significantly different from those of the control sample ($P > 0.05$), where the swelling power was $4,141.8 \pm 305.41\%$ and swelling capacity was 52.71 ± 1.37 g/mL (Supplementary Table 2). However, the trend shows that the swelling capacity tended to rise as the freezing time and freezing cycles were increased (Table 3). The swelling capacity of a substance can be associated with its hydration capacity, which is mainly correlated with the number of hydroxyl groups in molecules (Yang et al., 2021). The increase in the swelling capacity of glucomannan gel is an indication that a higher amount of water can be entrapped within the matrix of glucomannan chains.

The results showed that the swelling power of the treated samples was inclined to increase when the freezing time was increased (Table 4). Since swelling power refers to the capability of a component to move due to water facilitation (Reshu et al., 2017), the high swelling power of the treated samples can be an indication that more fragments of glucomannan chains move and bind with more volume of water. Moreover, Liu et al. (2019) reported that FTC pre-treatments have the ability to produce porous starch, which shows high swelling power properties. In this context, the high swelling power of the treated samples might also be caused by the high porosity of the glucomannan molecules. Results of the morphological properties (Figure 2) showed that the FTC pre-treatments increased the porosity on the glucomannan surfaces.

Table 3. The color of glucomannan.

	L			a			b		
	F2	F4	F6	F2	F4	F6	F2	F4	F6
S1	62.28±0.01 ^{Aa}	61.60±0.01 ^{Ba}	62.06±0.01 ^{Ca}	7.62±0.01 ^{Ac}	8.27±0.14 ^{Bc}	8.14±0.02 ^{Cc}	14.00±0.01 ^{Ad}	15.20±0.02 ^{Bd}	15.56±0.02 ^{Cd}
S2	63.09±0.00 ^{Ab}	62.82±0.03 ^{Bb}	60.78±0.00 ^{Cb}	7.18±0.01 ^{Ab}	8.00±0.01 ^{Bb}	7.79±0.01 ^{Cb}	13.94±0.01 ^{Ac}	15.07±0.01 ^{Bc}	15.00±0.01 ^{Cc}
S3	64.80±0.01 ^{Ac}	60.09±0.00 ^{Bc}	61.39±0.00 ^{Cc}	6.96±0.02 ^{Aa}	7.92±0.02 ^{Ba}	7.44±0.01 ^{Ca}	13.86±0.01 ^{Ab}	14.98±0.01 ^{Bb}	14.14±0.01 ^{Cb}
S4	64.74±0.02 ^{Ad}	61.76±0.02 ^{Bd}	61.51±0.00 ^{Cd}	6.96±0.02 ^{Aa}	7.78±0.02 ^{Ba}	7.56±0.02 ^{Ca}	14.19±0.01 ^{Aa}	14.48±0.01 ^{Ba}	14.26±0.01 ^{Ca}

*The average value marked by different letter notations showed a noticeable difference according to further tests of Duncan at a real level of 5%. Capital letter notation is read vertically, and lowercase notation is read horizontally; F: freezing time (F2: 2 days, F4: 4 days, and F6: 6 days); S: cycle number (S1: 1 cycle, S2: 2 cycles, S3: 3 cycles, and S4: 4 cycles).

Table 4. Viscosity and swelling properties of glucomannan*.

	Viscosity (cP)			Swelling Capacity (g/ml)			Swelling Power (%)		
	F2	F4	F6	F2	F4	F6	F2	F4	F6
S1	1,680±8 ^{Ac}	9,245±191 ^{Bc}	4,842±178 ^{Bc}	52.0±1.8 ^{Ab}	51.7±0.0 ^{Bb}	51.8±0.1 ^{Bb}	3,565.0±38.9 ^{Ad}	3,252.7±84.7 ^{Ad}	4,000.8±45 ^{Bd}
S2	1,150±23 ^{Ab}	4,148±166 ^{Bb}	4,569±47 ^{Bb}	49.1±0.1 ^{Aa}	51.2±0.2 ^{Ba}	52.1±1.3 ^{Ba}	3,213.6±154 ^{Ac}	2,926.8±74.4 ^{Ac}	3,698.7±29.3 ^{Bc}
S3	5,580±161 ^{Ab}	266±0 ^{Bb}	4,500±0 ^{Bb}	48.8±0.8 ^{Ab}	51.2±0.1 ^{Bab}	53.6±0.4 ^{Bab}	2,734.2±0.8 ^{Ab}	3,095.7±47.4 ^{Ab}	3,346.6±7.2 ^{Bb}
S4	2,942±246 ^{Aa}	2,582±202 ^{Ba}	1,994±65 ^{Ba}	48.8±0.3 ^{Ab}	53.3±0.3 ^{Bab}	51.9±0.0 ^{Bab}	2,690.3±9.1 ^{Aa}	2,917.9±146.1 ^{Aa}	3,040.4±56.7 ^{Ba}

*The average value marked by different letter notations showed a noticeable difference according to further tests of Duncan at a real level of 5%. Capital letter notation is read vertically, and lowercase notation is read horizontally.

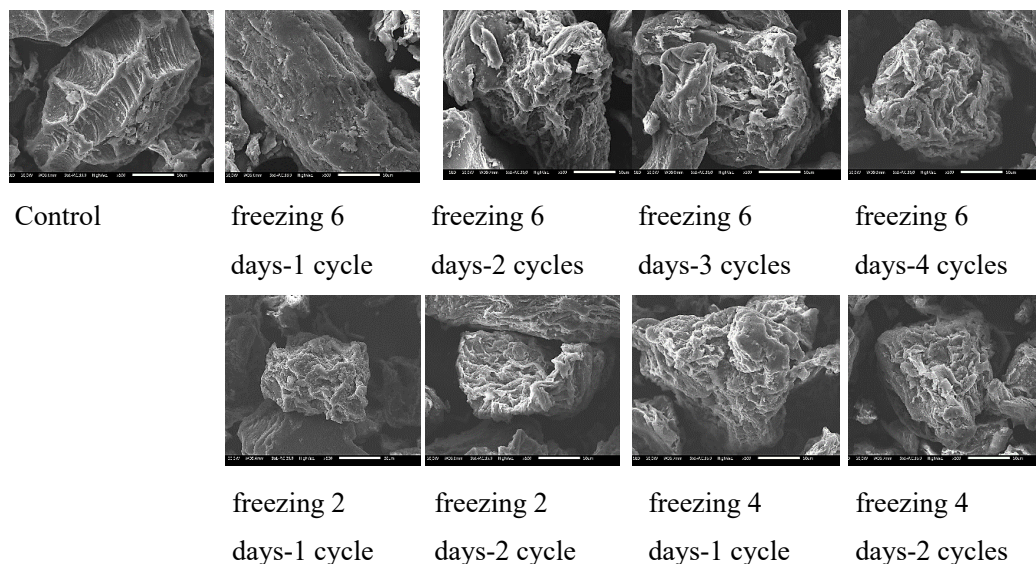


Figure 2. Morphological properties of the control and FTC treated samples observed with 500× magnifications.

3.4. Morphological properties

The morphological properties of the control and the treated samples are exhibited in Figure 2. The surface of the FTC-treated sample after 6 days of freezing-1 cycle is almost identical to that of the control sample. They showed relatively smooth surfaces with globular shapes. Generally, glucomannan molecules are located within the matrix of protein, cellulose, starch, and the other components building cell walls (Yanuriati & Basir, 2020). The smooth surface of glucomannan globes can be an indication that other components have been released during the glucomannan extraction process (Yanuriati & Basir, 2020). Figure 2 also indicates that the FTC pre-treatments caused damage and fractures on the surface of glucomannan molecules. The growth of ice followed by the ice melting repeatedly during freezing-thawing cycles has the capability to destroy the microstructure of the glucomannan matrix (Liu et al., 2019). Figure 2 also reveals that increasing the number of freezing cycles caused the surface of glucomannan molecules to be more porous and rougher. The rough and porous surfaces of the glucomannan molecules might cause higher values of the swelling properties of the FTC-treated samples than the control samples (Supplementary Tables 1 and 2).

3.5. Molecular weight distribution

The molecular weight distribution of glucomannan samples from FTC pre-treatments is shown in Table 5. The results showed that the molecular weight reduced at freezing for 2 and 4 days, and the PDI increased at freezing for 4 and 6 days. The PDI of glucomannan from FTC pre-treatment was higher than that of untreated glucomannan (Yanuriati et al., 2017). This result implied that the FTC pre-treatments impacted the glucomannan chain length. The higher value of PDI indicated the glucomannan degradation polymer because of the ice crystal growth during the freezing process (Feng et al., 2021). The growth of ice crystals could randomly destroy the structure

Table 5. Number-average M_n , Weight-average M_w , z-average M_z molecular weights, and poly-dispersity index (PDI) of samples.

Samples	M_n (Da)	M_w (Da)	PDI (M_w/M_n)
Control	7.60×10^5	2.22×10^6	2.93
Freezing (2 days)	5.68×10^5	1.57×10^6	2.77
Freezing (4 days)	4.78×10^5	1.84×10^6	3.85
Freezing (6 days)	9.75×10^5	3.77×10^6	3.87

of glucomannan, resulting in a higher PDI value (Li et al., 2021; Liu et al., 2022).

3.6. FTIR Spectra

The FTIR spectra of the control and the FTC-treated samples are displayed in Figures 3A, 3B, and 3C. It can be seen that there are no differences in the patterns of the FTIR spectra of the control and the FTC-treated samples. The characteristic peaks of O-H stretching, C-H stretching, C=O stretching, C-H bending, and C-O-C stretching appeared at wavenumbers of 3,276, 2,880, 1,734, 1,378–1,164, and 1,004 cm^{-1} , respectively, which are similar to those that have been reported for commercial glucomannan (Felix da Silva et al., 2020; Kurt & Kahyaoglu, 2017). The OH group of glucomannan monomers, including glucose and mannose, appeared at 3,200–3,500 cm^{-1} . Other identity peaks of the monomers, including C-H stretching, C-H bending, and C-O-C stretching, were detected at 2,880, 1,378–1,164, and 1,004 cm^{-1} , respectively, which have also been previously reported (Nurlela et al., 2020).

3.7. X-Ray Diffraction

Figure 3D displayed the XRD patterns of the control and the FTC-treated samples. All samples exhibited the pattern of amorphous structures of glucomannan chains in which no crystalline peaks appeared. Since glucomannan molecules are built by the

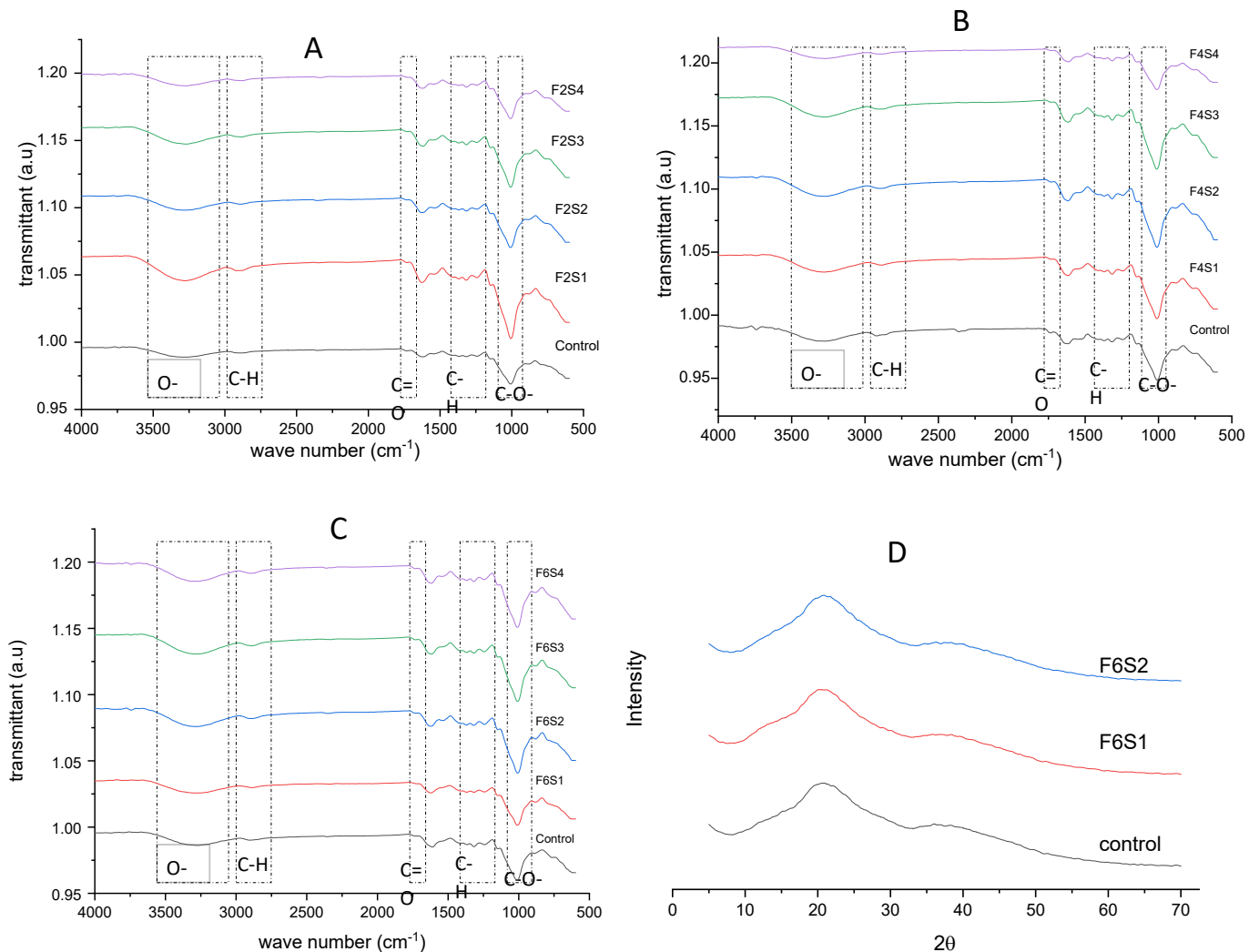


Figure 3. FTIR spectra of extracted glucomannan: (A) freezing in 6 days; (B) freezing in 4 days; (C) freezing in 2 days; (D) X-ray diffraction patterns of extracted glucomannan.

random entanglements of glucomannan chains, no crystalline structures are constructed (Kurt & Kahyaoglu, 2017; Liu et al., 2019). This result indicated that the FTC pre-treatments did not create crystalline structures in glucomannan chains. This result also emphasized that the starch granules had been removed from the matrix of the control and treated samples during the glucomannan extraction process.

4. Conclusion

The FTC pre-treatment significantly affected the physico-chemical properties of the glucomannan samples except for their protein and calcium oxalate content. Dunnett's comparative test showed that the ash and glucomannan content and the color properties of the treated samples were significantly different from the control. The smooth surface of the spherical glucomannan molecule becomes more porous due to surface damage due to the growth of ice crystals and melting during the freezing and thawing processes. Since FTC pre-treatments tended to reduce the glucomannan and starch contents, further

studies are needed to optimize the FTC pre-treatment in order to obtain porang flour with high glucomannan and low impurity contents. FTIR spectra and XRD patterns confirmed that other components of porang flour besides glucomannan were removed from the control and treatment samples during the glucomannan extraction process.

References

- Abedi, E., Sayadi, M., & Pourmohammadi, K. (2022). Food Hydrocolloids Effect of freezing-thawing pre-treatment on enzymatic modification of corn and potato starch treated with activated α -amylase: Investigation of functional properties. *Food Hydrocolloids*, 129, 107676. <https://doi.org/10.1016/j.foodhyd.2022.107676>
- Anwar, M., McConnell, M., & Bekhit, A. E. D. (2021). New freeze-thaw method for improved extraction of water-soluble non-starch polysaccharide from taro (*Colocasia esculenta*): Optimization and comprehensive characterization of physico-chemical and structural properties. *Food Chemistry*, 349, 129210. <https://doi.org/10.1016/j.foodchem.2021.129210>

- Chairiyah, N., Harijati, N., & Mastuti, R. (2016). Variation of Calcium Oxalate (CaOx) Crystals in Porang Corms (*Amorphophallus muelleri* Blume) at Different Harvest Time. *American Journal of Plant Sciences*, 7(2), 306-315. <https://doi.org/10.4236/ajps.2016.72030>
- Charoenrein, S., & Owcharoen, K. (2016). Effect of freezing rates and freeze-thaw cycles on the texture, microstructure and pectic substances of mango. *International Food Research Journal*, 23(2), 613-620.
- Chua, M., Chan, K., Hocking, T. J., Williams, P. A., Perry, C. J., & Baldwin, T. C. (2012). Methodologies for the extraction and analysis of konjac glucomannan from corms of *Amorphophallus konjac* K. Koch. *Carbohydrate Polymers*, 87(3), 2202-2210. <https://doi.org/10.1016/j.carbpol.2011.10.053>
- Chua, M., Hocking, T. J., Chan, K., & Baldwin, T. C. (2013). Temporal and spatial regulation of glucomannan deposition and mobilization in corms of a morphophallus konjac (Araceae). *American Journal of Botany*, 100(2), 337-345. <https://doi.org/10.3732/ajb.1200547>
- Dwiyono, K., & Djauhari, M. A. (2019). *Indonesian Konjac: Its Benefit in Industry and Food Security*.
- Faridah, A., & Widjanarko, S. B. (2013). Optimization of Multilevel Ethanol Leaching Process of Porang Flour (*Amorphophallus muelleri*) Using Response Surface Methodology. *International Journal on Advanced Science, Engineering and Information Technology*, 3(2), 172-178. <https://doi.org/10.18517/ijaseit.3.2.309>
- Faridah, A., Widjanarko, S. B., & Sutrisno, A. (2012). Optimization of Increasing Glucomannan Levels and Decreasing Calcium Oxalate in the Flourishing Process of Porang Chips (*Amorphophallus oncophyllus*) with the Mechanical Method. In National Seminar of PATPI 2011, Manado.
- Felix da Silva, D., Ogawa, C. Y. L., Sato, F., Neto, A. M., Larsen, F. H., & Matumoto-Pintro, P. T. (2020). Chemical and physical characterization of Konjac glucomannan-based powders by FTIR and ¹³C MAS NMR. *Powder Technology*, 361, 610-616. <https://doi.org/10.1016/j.powtec.2019.11.071>
- Feng, X., Dai, H., Ma, L., Fu, Y., Yu, Y., Zhu, H., Wang, H., Sun, Y., Tan, H., & Zhang, Y. (2021). Effect of freezing temperature on molecular structure and functional properties of gelatin extracted by microwave-freezing-thawing coupling method. *Food Science and Technology*, 149, 111894. <https://doi.org/10.1016/j.lwt.2021.111894>
- Feng, X., Liu, T., Ma, L., Dai, H., Fu, Y., Yu, Y., Zhu, H., Wang, H., Tan, H., & Zhang, Y. (2022). A green extraction method for gelatin and its molecular mechanism. *Food Hydrocolloids*, 124(Part B), 107344. <https://doi.org/10.1016/j.foodhyd.2021.107344>
- Food and Agriculture Organization (FAO). (1996). *Konjac flour* (v. 4, Issue 1996). Retrieved from http://www.fao.org/fileadmin/user_upload/jecfa_additives/docs/Monograph1/additive-245-m1.pdf
- Jiang, M., Li, H., Shi, J.-S., & Xu, Z.-H. (2018). Depolymerized konjac glucomannan: preparation and application in health care. *Journal of Zhejiang University: Science B*, 19(7), 505-514. <https://doi.org/10.1631/jzus.B1700310>
- Kurt, A., & Kahyaoglu, T. (2017). Purification of glucomannan from salep: Part 2. Structural characterization. *Carbohydrate Polymers*, 169, 406-416. <https://doi.org/10.1016/j.carbpol.2017.04.052>
- Li, J., Liu, Z., Feng, C., Liu, X., Qin, F., Liang, C., Bian, H., Qin, C., & Yao, S. (2021). Green, efficient extraction of bamboo hemicellulose using freeze-thaw assisted alkali treatment. *Bioresource Technology*, 333, 125107. <https://doi.org/10.1016/j.biortech.2021.125107>
- Liu, M., Ma, H., Liang, Y., Sun, L., Li, J., Dang, W., Li, L., & Zheng, X. (2022). Effect of multiple freezing / thawing cycles on the physicochemical properties and structural characteristics of starch from wheat flours with different gluten strength. *International Journal of Biological Macromolecules*, 194, 619-625. <https://doi.org/10.1016/j.ijbiomac.2021.11.105>
- Liu, Y., Gao, J., Wu, H., Gou, M., Jing, L., Zhao, K., Zhang, B., Zhang, G., & Li, W. (2019). Molecular, crystal and physicochemical properties of granular waxy corn starch after repeated freeze-thaw cycles at different freezing temperatures. *International Journal of Biological Macromolecules*, 133, 346-353. <https://doi.org/10.1016/j.ijbiomac.2019.04.111>
- Ma, S., Zhu, P., Wang, M., Wang, F., & Wang, N. (2019). Effect of konjac glucomannan with different molecular weights on physicochemical properties of corn starch. *Food Hydrocolloids*, 96, 663-670. <https://doi.org/10.1016/j.foodhyd.2019.06.014>
- Mortensen, A., Aguilar, F., Crebelli, R., Di Domenico, A., Frutos, M. J., Galtier, P., Gott, D., Gundert-Remy, U., Lambré, C., Leblanc, J., Lindtner, O., Moldeus, P., Mosesso, P., Oskarsson, A., Parent-Massin, D., Stankovic, I., Waalkens-Berendsen, L., Woutersen, R. A., Wright, M., Dusemund, B. (2017). Re-evaluation of konjac gum (E 425 i) and konjac glucomannan (E 425 ii) as food additives. *EFSA Journal*, 15(6), e04864. <https://doi.org/10.2903/j.efsa.2017.4864>
- National Standardization Agency (1992). *SNI 01-2891-1992: Testing methods of food and beverage*. National Standardization Agency.
- Noonan, S. C. (1999). Oxalate content of foods and its effect on humans. *Asia Pacific Journal of Clinical Nutrition*, 8(1), 64-74. <https://doi.org/10.1046/j.1440-6047.1999.00038.x>
- Nurlela, N., Andriani, D., & Arizal, R. (2020). Extraction of Glucomannan from porang (*Amorphophallus muelleri* Blume) flour using Ethanol. *Jurnal Sains Dan Terapan Kimia*, 14(2), 88-98. <https://doi.org/10.20527/jst.v14i2.8330>
- Nurlela, N., Ariesta, N., Santosa, E., & Muhandri, T. (2019). Effect of harvest timing and length of storage time on glucomannan content in porang tubers. *IOP Conference Series: Earth and Environmental Science*, 299(1), 1-8. <https://doi.org/10.1088/1755-1315/299/1/012012>
- Peiying, L., (2003). *Konjac*. China Agriculture Press, 298 p.
- Peiying, L., Shenglin, Z., Guohua, Z., Yan, C., Huaxue, O., Mei, H., Zhongfeng, W., Wei, X., Hongy, P., Zhang Shenglin, Z., Guohua, C. Y., Huaxue, O., Mei, H., & Zhongfeng, W. (2002). *Professional Standard of the People's Republic of China for Konjac flour*.
- Phothiset, S., & Charoenrein, S. (2014). Effects of freezing and thawing on texture, microstructure and cell wall composition changes in papaya tissues. *Journal of the Science of Food and Agriculture*, 94(2), 189-196. <https://doi.org/10.1002/jsfa.6226>
- Reshu, M. S., Chagam, R., Reddy, K., & Haripriya, S. (2017). Functional and physicochemical characteristics of cookies prepared from *Amorphophallus paeoniifolius* flour. *Journal of Food Science and Technology*, 54(7), 2156-2165. <https://doi.org/10.1007/s13197-017-2656-y>
- Shen, G., Zhang, L., Hu, T., Li, Z., Chen, A., Zhang, Z., Wu, H., Li, S., & Hou, X. (2020). Preparation of potato flour by freeze-thaw pretreatment: Effect of different thawing methods on hot-air drying process and physicochemical properties. *Food Science and Technology*, 133, 110157. <https://doi.org/10.1016/j.lwt.2020.110157>
- Shenglin, Z., Purwadaria, H. K., Borompichaichartkul, C., & Tripetch, P. (2020). Konjac Industry in Major Producing Countries. In Z. Shenglin, H. K. Purwadaria, C. Borompichaichartkul & P. Tripetch (eds.), *Konjac Glucomannan* (p. 223-254). Taylor & Francis Group. <https://doi.org/10.4324/9780429429927-9>
- Shi, X.-D., Yin, J. Y., Cui, S. W., Wang, Q., Wang, S. Y., & Nie, S. P. (2020a). Comparative study on glucomannans with different structural characteristics : Functional properties and intestinal production of short chain fatty acids. *International Journal of Biological Macromolecules*, 164, 826-835. <https://doi.org/10.1016/j.ijbiomac.2020.07.186>

- Shi, X.-D., Yin, J. Y., Cui, S. W., Wang, Q., Wang, S. Y., & Nie, S. P. (2020b). Plant-derived glucomannans: Sources, preparation methods, structural features, and biological properties. *Trends in Food Science and Technology*, 99, 101-116. <https://doi.org/10.1016/j.tifs.2020.02.016>
- Sulaiman, I., Noviasari, S., Lubis, Y. M., Rozali, Z. F., Eriani, K., & Asriza, C. W. (2020). Analysis types and functions of microbes and duration of fermentation in the process of reducing levels of concentration oxalate levels in taro Kimpul. *Systematic Reviews in Pharmacy*, 11(11), 1450-1456. <https://doi.org/10.31838/srp.2020.11.205>
- Tao, H., Huang, J. S., Xie, Q. T., Zou, Y. M., Wang, H. L., Wu, X. Y., & Xu, X. M. (2018). Effect of multiple freezing-thawing cycles on structural and functional properties of starch granules isolated from soft and hard wheat. *Food Chemistry*, 265, 18-22. <https://doi.org/10.1016/j.foodchem.2018.05.065>
- Tao, H., Yan, J., Zhao, J., Tian, Y., Jin, Z., & Xu, X. (2015). Effect of multiple freezing/thawing cycles on the structural and functional properties of waxy rice starch. *PLoS One*, 10(5), e0127138. <https://doi.org/10.1371/journal.pone.0127138>
- Tu, J., Zhang, M., Xu, B., & Liu, H. (2015). Effects of different freezing methods on the quality and microstructure of lotus (*Nelumbo nucifera*) root. *International Journal of Refrigeration*, 52, 59-65. <https://doi.org/10.1016/j.ijrefrig.2014.12.015>
- van der Sman, R. G. M. (2020). Impact of Processing Factors on Quality of Frozen Vegetables and Fruits. *Food Engineering Reviews*, 12(4), 399-420. <https://doi.org/10.1007/s12393-020-09216-1>
- Wardhani, D. H., Nugroho, F., & Muslihuddin, M. (2015). Extraction of glucomannan of porang tuber (*Amorphophallus onchophyllus*) by using IPA. *AIP Conference Proceedings*, 1699, 060007. <https://doi.org/10.1063/1.4938361>
- Widjanarko, S. B., Widyastuti, E., & Rozaq, F. I. (2015). The effect of porang (*Amorphophallus muelleri* blume) milling time using ball mill (cyclone separator) method toward physical and chemical properties of porang flour. *Jurnal Pangan Dan Agroindustri*, 3(3), 867-877.
- Xu, K., Chi, C., She, Z., Liu, X., Zhang, Y., Wang, H., & Zhang, H. (2022). Understanding how starch constituent in frozen dough following freezing-thawing treatment affected quality of steamed bread. *Food Chemistry*, 366, 130614. <https://doi.org/10.1016/j.foodchem.2021.130614>
- Yang, Y., Zheng, S., Li, Z., Pan, Z., Huang, Z., Zhao, J., & Ai, Z. (2021). Influence of three types of freezing methods on physicochemical properties and digestibility of starch in frozen unfermented dough. *Food Hydrocolloids*, 115, 106619. <https://doi.org/10.1016/j.foodhyd.2021.106619>
- Yanuriati, A., & Basir, D. (2020). (*Amorphophallus muelleri* blume) glucomannan solubility increase by wet dan dry milling. *AgriTECH*, 40(3), 223-231. <https://doi.org/10.22146/agritech.43684>
- Yanuriati, A., Marseno, D. W., Rochmadi, & Harmayani, E. (2017). Characteristics of glucomannan isolated from fresh tuber of Porang (*Amorphophallus muelleri* Blume). *Carbohydrate Polymers*, 156, 56-63. <https://doi.org/10.1016/j.carbpol.2016.08.080>
- Yao-ling, L., Rong-hua, D., Ni, C., Juan, P., & Jie, P. (2013). Review of Konjac Glucomannan: Isolation, Structure, Chain Conformation and Bioactivities. *Journal of Single Molecule Research*, 1(1), 7-14. <https://doi.org/10.12966/jmsr.07.03.2013>
- Yu, H., Mei, J., & Xie, J. (2022). New ultrasonic assisted technology of freezing, cooling and thawing in solid food processing: A review. *Ultrasonics Sonochemistry*, 90, 106185. <https://doi.org/10.1016/j.ultsonch.2022.106185>
- Zhang, M., Li, F., Diao, X., Kong, B., & Xia, X. (2017). Moisture migration, microstructure damage and protein structure changes in porcine longissimus muscle as influenced by multiple freeze-thaw cycles. *Meat Science*, 133, 10-18. <https://doi.org/10.1016/j.meatsci.2017.05.019>
- Zhao, J., Zhang, D., Srzednicki, G., Kanlayanarat, S., & Borompichaichartkul, C. (2010). Development of a low-cost two-stage technique for production of low-sulphur purified konjac flour. *International Food Research Journal*, 17(4), 1113-1124.
- Zhao, L., Li, L., Liu, G. Q., Chen, L., Liu, X., Zhu, J., & Li, B. (2013). Effect of freeze-thaw cycles on the molecular weight and size distribution of gluten. *Food Research International*, 53(1), 409-416. <https://doi.org/10.1016/j.foodres.2013.04.013>